Research
Applied Geophysics—Article

Imposing Active Sources during High-Frequency Passive Surface-Wave Measurement

Feng Cheng [a], Jianghai Xia [b,*], Chao Shen [c], Yue Hu [a], Zongbo Xu [d], Binbin Mi [a]

[a] Subsurface Imaging and Sensing Laboratory, Institute of Geophysics and Geomatics, China University of Geosciences, Wuhan 430074, China
[b] School of Earth Sciences, Zhejiang University, Hangzhou 310027, China
[c] School of Measurement and Testing Engineering, China Jiliang University, Hangzhou 310018, China
[d] Department of Geosciences, Boise State University, Boise, ID 83725, USA

ARTICLE INFO

ABSTRACT

Passive surface-wave utilization has been intensively studied as a means of compensating for the shortage of low-frequency information in active surface-wave measurement. In general, passive surface-wave methods cannot provide phase velocities up to several tens of hertz; thus, active surface-wave methods are often required in order to increase the frequency range. To reduce the amount of field work, we propose a strategy for a high-frequency passive surface-wave survey that imposes active sources during continuous passive surface-wave observation; we call our strategy "mixed-source surface-wave (MSW) measurement." Short-duration (within 10 min) passive surface waves and mixed-source surface waves were recorded at three sites with different noise levels: namely, inside a school, along a road, and along a railway. Spectral analysis indicates that the high-frequency energy is improved by imposing active sources during continuous passive surface-wave observation. The spatial autocorrelation (SPAC) method and the multichannel analysis of passive surface waves (MAPS) method based on cross-correlations were performed on the recorded time sequences. The results demonstrate the flexibility and applicability of the proposed method for high-frequency phase velocity analysis. We suggest that it will be constructive to perform MSW measurement in a seismic investigation, rather than exclusively performing either active surface-wave measurement or passive surface-wave measurement.

1. Introduction

Surface-wave methods are increasingly used as non-destructive, noninvasive, inexpensive, and accurate seismic-imaging methods in multiscale engineering and geological applications. In order to obtain an objective investigation depth and specific resolution, the frequencies of surface waves are critical for geotechnical applications due to their dispersive properties. The capability of sources to generate low-frequency surface waves with deeper penetration has recently been a subject of increasing interest [1].

Two types of sources—active and passive—are generally used in surface-wave measurements. Common examples of active sources include a hammer, a dropped weight, and a harmonic shaker. Utilizing an active seismic source, the multichannel analysis of

surface waves (MASW) method [2–6] can directly determine phase velocities from multichannel surface-wave data after transforming waveform data from the time-offset (t-x) domain into the frequency-velocity (f-v) domain. To increase the lateral resolution of surface-wave methods in heterogeneous environments, Hayashi and Suzuki [7] applied common midpoint cross-correlation analysis to MASW. Due to the difficulty in generating low-frequency energy, however, reasonably portable active sources are often limited in their ability to sample deep soils.

Passive surface waves such as those of microseisms (< 0.6 Hz, ocean-generated natural noise) and microtremors (> 1 Hz, cultural noise such as vehicle traffic, railways, or machinery) are typically of lower frequency. Therefore, passive surface-wave measurement would provide a wide range of penetration depths and, as a result, strong motivation to utilize such measurements. In fact, passive surface-wave utilization such as the microtremor survey method, which utilizes surface waves recorded at earthquake stations [8], has been intensively studied in Japan. Using microtremors and

assuming a dominant Rayleigh-wave energy contribution, shear-wave velocity (V_s) can be derived by the inversion of spatial auto-correlation curves [9–11]. Louie [12] presented the refraction microtremor method as a fast and effective passive seismic method based on the τ-p transformation, or slant-stacking. Park et al. [13] introduced a strategy that combined the imaging dispersion of passive surface waves with an active scheme based on phase-shifts measurement. Cheng et al. [14] improved this passive surface-wave method with azimuthal adjustment based on cross-correlations, resulting in the method known as multichannel analysis of passive surface waves (MAPS).

In addition, active and passive measurements have been combined in order to extend the investigation depth of surface waves without sacrificing near-surface resolution [1,11,15–17]. However, when these two kinds of measurements (i.e., dispersion images or curves) are roughly combined together, the result can be potentially inappropriate for further analysis, for two reasons: ① The spatial resolution of the combined inverted V_s will be ambiguous, because the spatial sampling interval in passive surface-wave measurement is usually several—or even ten—times greater than the interval used in active surface-wave measurement; and ② passive and active measurements can show a large discrepancy in the overlapping frequency range, because phase velocities that are determined through active measurement usually appear slower due to insufficient information in the low-frequency range [18], whereas passive measurement are interfered with by higher modes, aliasing, and body waves in the high-frequency range.

If passive surface-wave methods are able to provide phase velocities up to several tens of hertz, then the active surface-wave method may not be necessary, and the amount of field work can be dramatically reduced. In this study, we propose a combined active-passive surface-wave method that imposes active sources during continuous passive surface-wave observation in order to obtain high-frequency passive surface-wave measurement; we call this kind of recording, which consists of passive surface waves (e.g., microtremors) and an active-source shot, "mixed-source surface-wave (MSW) measurement." Passive surface-wave measurement using the spatial autocorrelation (SPAC) and MAPS methods, as well as active surface-wave measurement, were performed at three sites with different noise levels: namely, inside a school, along a road, and along a railway. As a preliminary work, the results presented here demonstrate the feasibility of the proposed combined active-passive surface-wave method in further extending the frequency band of passive surface-wave measurement.

2. Passive surface-wave methods

2.1. Spatial autocorrelation

Aki [9,19] proposed a technique to determine a phase velocity dispersion curve from microtremors recorded by a seismic array. He established that the SPAC coefficient $\rho(r, w)$, as a function of frequency for a given interstation distance, r, and angular frequency, w, averaged over many different azimuths, can be written as follows:

$$\rho(r, w) = J_0\left(\frac{rw}{c}\right) \tag{1}$$

where J_0 is the zero-order Bessel function of the first kind and c is the phase velocity at frequency w at the site. The wavefield is assumed to consist of surface waves propagating with equal power in all directions. The phase velocity for each frequency can be obtained by inverting the observed SPAC coefficients. A common way of obtaining the phase velocity is to ensemble-average the observed cross-spectra and normalize the cross-spectra by the averaged power-spectra [20]. Weemstra et al. [21] normalized the

cross-spectra before the ensemble-average and obtained the SPAC coefficient as follows:

$$\rho(r, w) = \left\langle \frac{\Re[u(x_1, w)u^*(x_2, w)]}{|u(x_1, w)| \, |u(x_2, w)|} \right\rangle \tag{2}$$

where $\langle \cdot \rangle$ denotes the ensemble-average; $\Re[\cdot]$ takes the real part of a complex argument; and $u(x_k, w)$ is the power of the wavefield at the station x_k.

Following the theory developed by Aki [9] and further discussed by Asten [22], we use the SPAC coefficients to fit the zero-order Bessel function of the first kind (Eq. (1)) in order to perform an inversion to obtain a one-dimensional (1D) phase velocity dispersion curve by defining the fitting residual, ε, as follows:

$$\varepsilon(c_i, w_j) = \rho(r, w) - J_0\left(\frac{rw_j}{c_i}\right) \tag{3}$$

We then use a grid search over the phase velocity from 100 to 1000 m·s^{-1} and the frequency from 1 to 30 Hz in order to find the minimum L1-norm residual (step size 1 m·s^{-1} and 0.5 Hz, respectively).

In the ideal case of an isotropic noise wavefield, azimuthal averaging would not be needed in Eq. (2). For a real-world application, if the source distribution changes sufficiently over a certain time-span, then averaging over this time-span is similar to averaging over the azimuth for a fixed source distribution [23,24]. That means that it is possible to expand the applications of this method to a linear array with a fixed active source. The following applications will demonstrate the feasibility of this assumption.

2.2. Multichannel analysis of passive surface waves

The MASW scheme has been applied to roadside traffic noise in order to determine low-frequency dispersion information [13]. In order to reduce azimuthal effects and spatial aliasing in passive surface-wave measurement, Cheng et al. [14] improved this method with cross-correlations. In this preliminary work, only the inline plane-wave propagation case (Fig. 1) will be taken into account for the following field-data application. Interested readers are also referred to the articles cited in Ref. [14]. Receivers were installed on the road shoulder and used to detect plane waves propagating in the pavement. The active sources were imposed at the end of the receiver line. Our expectation was that high-frequency energy would be detected and improved by imposing active sources during continuous passive surface-wave (e.g., traffic noise) observation.

According to Cheng et al. [14], the relative dispersion energy matrix in the inline plane-wave propagation case can be calculated as follows:

$$E(f, v) = \left| \sum_{j=1}^{N-1} \sum_{k=j+1}^{N} \exp\left(\frac{i2\pi f x_{jk}}{v}\right) \frac{C_{jk}^+(f) + C_{jk}^-(f)}{2} \right| \tag{4}$$

where $E(f, v)$ is the relative dispersion energy matrix for a particular frequency f and a scanning phase velocity v; $C_{jk}^+(f)$ and $C_{jk}^-(f)$ are the Fourier transformation of the causal and the acausal parts of the
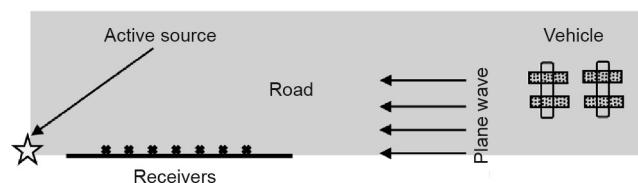

Fig. 1. Inline plane-wave propagation with active source imposing.

cross-correlation between traces j and k of the whitened records, respectively; x_{jk} corresponds to the distance between traces j and k; and N is the total trace number.

To improve the quality of the relative dispersion energy matrix, we followed the seismic noise interferometry processing described by Cheng et al. [25], which contains single-station data preparation (splitting, removing mean, removing trend, band-pass filter, temporal normalization, and spectral normalization), cross-correlation between a pair of stations, and signal to noise ratio (SNR) weighted stacking.

3. MSW measurement at three sites

As described above, the SPAC method and the MAPS method were applied to three sites: namely, inside a school, along a road, and along a railway. We roughly classified the passive surface waves (e.g., traffic noise) in the common urban areas into three levels: light (L), moderate (M), and strong (S). The three field-data examples can be regarded as the corresponding representations of these three noise levels. In this section, we describe how to impose active sources for MSW measurement, and examine its applicability to high-frequency phase velocity analysis.

3.1. Site 1: L-level passive surface waves

A combined active-passive surface-wave experiment was performed in the backyard of the Institute of Geophysics and Geomatics at the China University of Geosciences, in the city of Wuhan, China (Fig. 2). A 48-channel active-source shot gather was collected. The source was a 6.3 kg hammer vertically impacting a 6 in (1 in = 2.54 cm) plate (the red rectangle in Fig. 2). Meanwhile, a comparable linear array with 15 RefTek digitizers (the red ellipse in Fig. 2) was synchronously deployed. Unfortunately, several digitizers were not connected well, and only nine digitizers worked well until the end of the experiment. All the receivers were 4.5 Hz vertical-component geophones. The trace intervals of the active and passive measurements were 0.5 and 1.5 m, respectively, and the sampling rates were 0.25 and 8.0 ms, respectively.

It is clear that the Rayleigh wave is fully developed and is recorded from 0.03 to 0.3 s in Fig. 3(a). The dispersion image (Fig. 3(b)) was generated by applying a high-resolution linear Radon transform [26] to the original active-source shot. The dispersion image indicates a good dispersion energy within the valid wavenumber zone restricted by the two dashed lines between the

Nyquist wavenumber $(1/(2 \cdot dx))$ and the minimum wavenumber $(1/(N \cdot dx))$. Obviously, the active surface-wave measurement is limited in its ability to sample deep soils (> 10 m) due to the lack of low-frequency (< 20 Hz) information.

To compensate for the shortage of low-frequency information in the active surface-wave measurement, the recorded passive surface waves were utilized and analyzed. Note that we separated the continuous time sequences into two 10 min subsets; the former subset consists exclusively of "quiet" passive surface waves, whereas the latter subset contains several active-source shots with a hammer—namely, MSW. Fig. 4 displays two typical 10 s time sequences for each of both subsets, respectively. An active-source shot event is noticeable in the right panel between 8.5 s and 9.0 s. The SPAC method was applied to both the preprocessed passive surface-wave data and the preprocessed MSW data. The obtained dispersion energy images (Fig. 5(a) and (b)) demonstrate

Fig. 2. Combined active-passive surface-wave experiment in the backyard of the Institute of Geophysics and Geomatics.
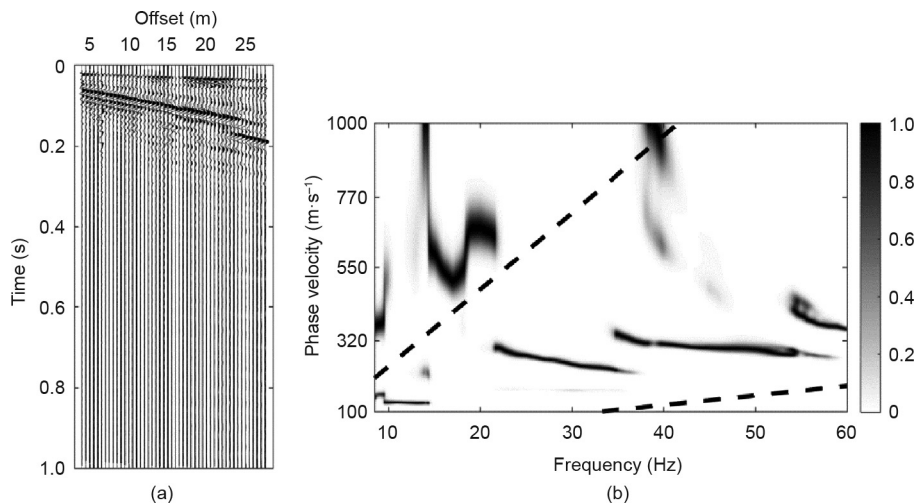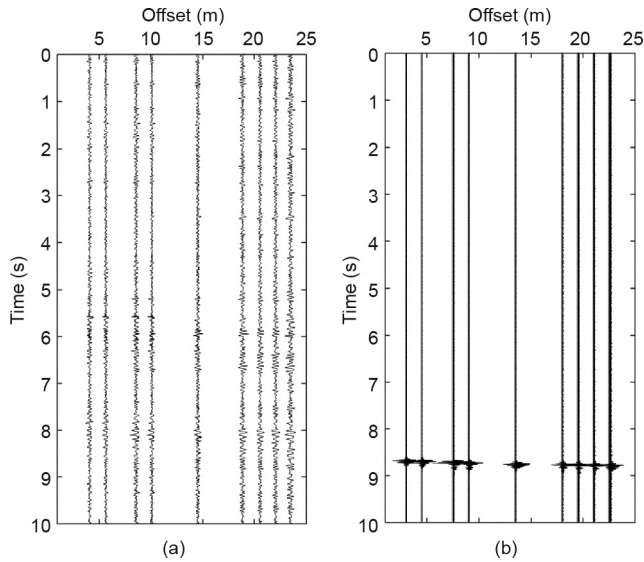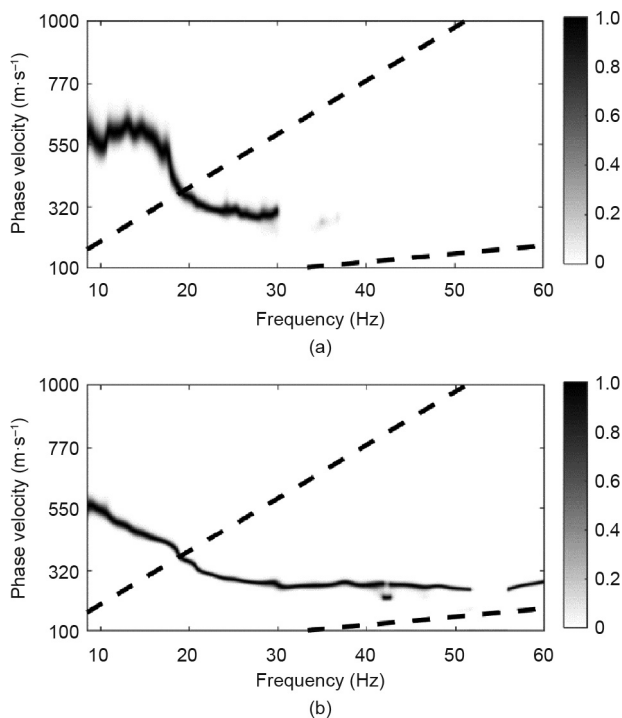

Fig. 3. (a) A shot gather with 48 vertical-component geophones of 4.5 Hz each at 0.5 m intervals with a sampling rate of 0.25 ms; (b) the normalized dispersion energy image.

Fig. 4. (a) One 10 s segment of the "quiet" passive surface waves over a 10 min period; (b) one 10 s segment of the MSW over a 10 min period.

Fig. 5. The obtained dispersion energy images using the SPAC method with (a) the "quiet" passive surface-wave data and (b) the mixed-source surface-wave data.

that passive surface-wave measurement is able to obtain dispersion information at lower frequencies. Moreover, they indicate that MSW measurement (Fig. 5(b)) extends the high-frequency limit of the original passive surface-wave measurement from 30 to 55 Hz (Fig. 5(a)). Thus, active surface-wave measurement fieldwork can be avoided, given the full-frequency band that is provided by MSW measurement.

Spectral analysis was performed in order to further demonstrate the feasibility of MSW measurement on high-frequency phase velocity analysis. The results indicate that imposing active sources during continuous passive surface-wave observation clearly improved the higher frequency energy of the recorded time sequences at this site (Fig. 6(a) and (b)), and consequently allows

the possibility of high-frequency dispersion analysis with MSW measurement. Compared with the MSW spectrum (Fig. 6(b)), the active surface-wave spectrum appears to be seriously distorted at low frequencies (< 15 Hz) (Fig. 6(c)).

We verified the accuracy of the passive surface-wave measurement using active surface-wave measurement. Because the fundamental model of active measurement in the high-frequency range (35 Hz < f < 55 Hz) is missing, we compared the passive measurement with the inverted active dispersion curve (black triangles in Fig. 7(a)). The largest misfit between the inverted active-source dispersion curve and the MSW measurement is about 7%, which demonstrates the accuracy of the proposed method. The picked dispersion curve (gray diamonds in Fig. 7(a)) was inverted to obtain the 1D V_s profile (as shown in Fig. 7(b)) using the Levenberg-Marquardt method [4,6,27,28].

3.2. Site 2: M-level passive surface waves

This test was carried out in the city of Changsha, China. A linear array of 12 vertical-component receivers of 2.5 Hz each was deployed on the road shoulder along the Xiaoxiang Road. The trace interval was fixed at 5 m and the sampling rate was 2 ms. The survey line parallels the river and road. To examine the effects of imposing active sources on passive surface-wave measurement, traffic noise was continuously recorded for 10 min and active sources were sequentially imposed five times during the last 5 min of the recording. The source was a 10 kg hammer vertically impacting a 6 in plate.

Fig. 8 shows two typical time sequences from 18 to 28 s for each of these two 5 min noise data subsets, respectively. Several linear events generated by vehicles can be distinguished in Fig. 8(a). An
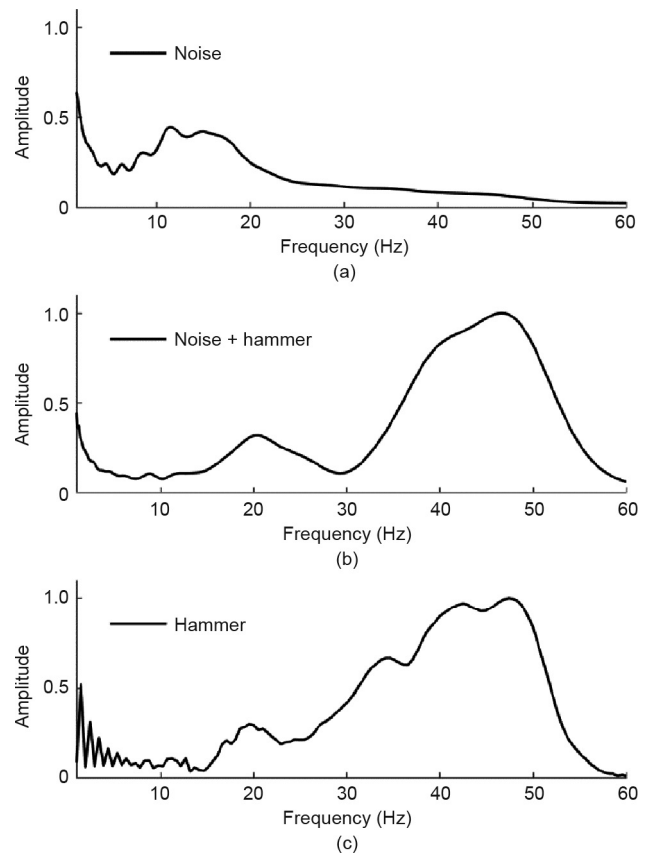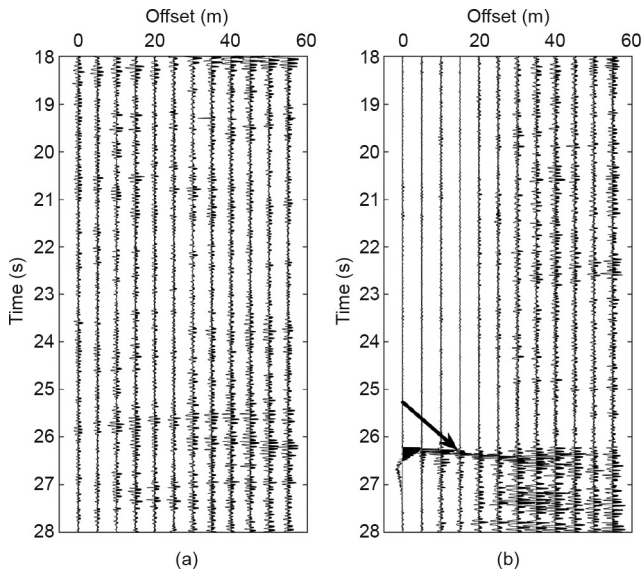

Fig. 6. Spectral analysis of (a) the "quiet" passive surface waves, (b) the MSW, and (c) the active shot gather. All of the average power spectra were normalized in the frequency band from 1 to 60 Hz.
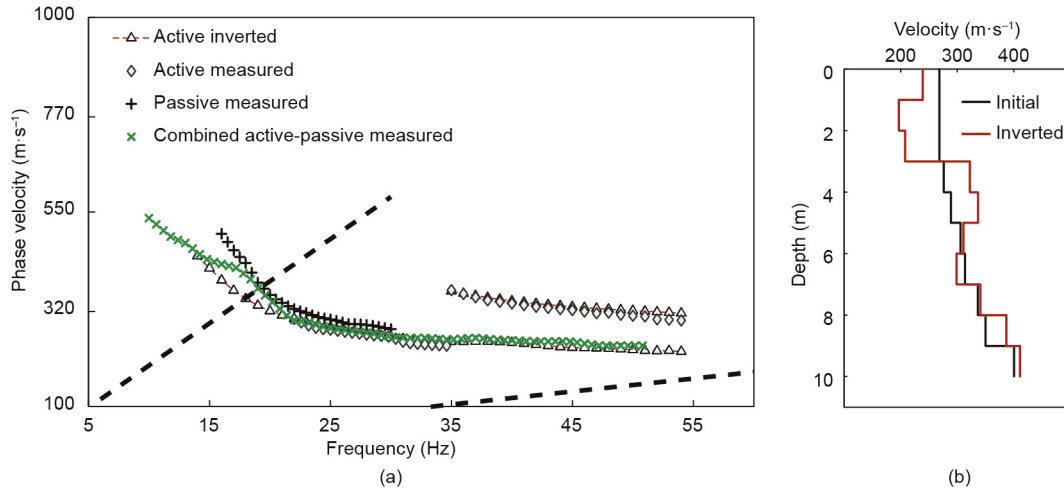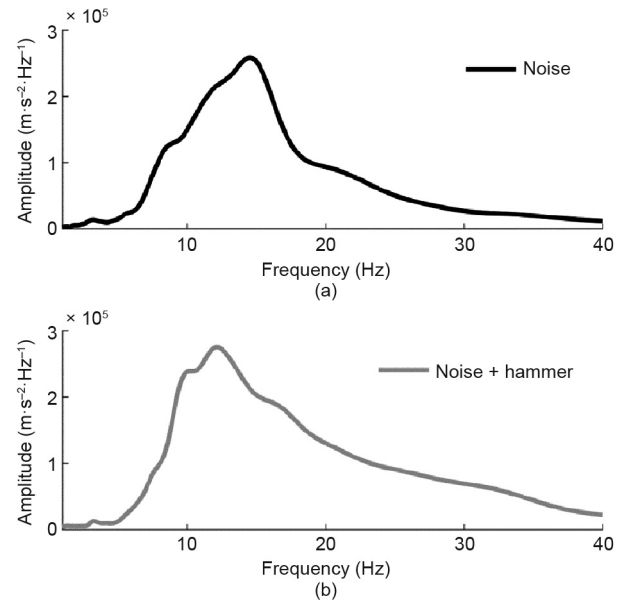
Fig. 7. (a) Comparison of the dispersion measurements for active (gray diamonds), passive (plus symbols), mixed-source (cross symbols), and inverted by active surface-wave measurement (black triangles); (b) inverted 1D V_s profile (the red line) and its initial model (the black line) by active surface-wave measurement.

active-source shot event is noticeable in Fig. 8(b) between 26 and 27 s, as the black arrow indicates, but suffers strong attenuation at the far offsets. Unlike the "quiet" environment at Site 1, the active surface-wave measurement gave a poor performance due to serious interference from traffic noise and the strong soil attenuation. We do not present it here. We also found that the imposed active sources did not significantly improve the high-frequency (> 20 Hz) energy, because the active-source energy was buried in the powerful traffic noise. However, compared with the absolute amplitude of the original passive surface wave (Fig. 9(a)), the absolute amplitude of the MSW (Fig. 9(b)) still appears to be generally higher, especially in the frequency range from 8 to 18 Hz.

The SPAC method (Fig. 10(a) and (b)) and MAPS method (Fig. 10(c) and (d)) were performed on both the passive surface-wave data and the MSW data. The acceptable dispersion curves of the above measurements (Fig. 10(e)) were picked out and fitted well with each other, which corroborated the validity of these measurements. Compared with the passive surface wave, the MSW presents better applicability for high-frequency (> 10 Hz) dispersion analysis. In addition, incoherent energy, which polluted the dispersion image
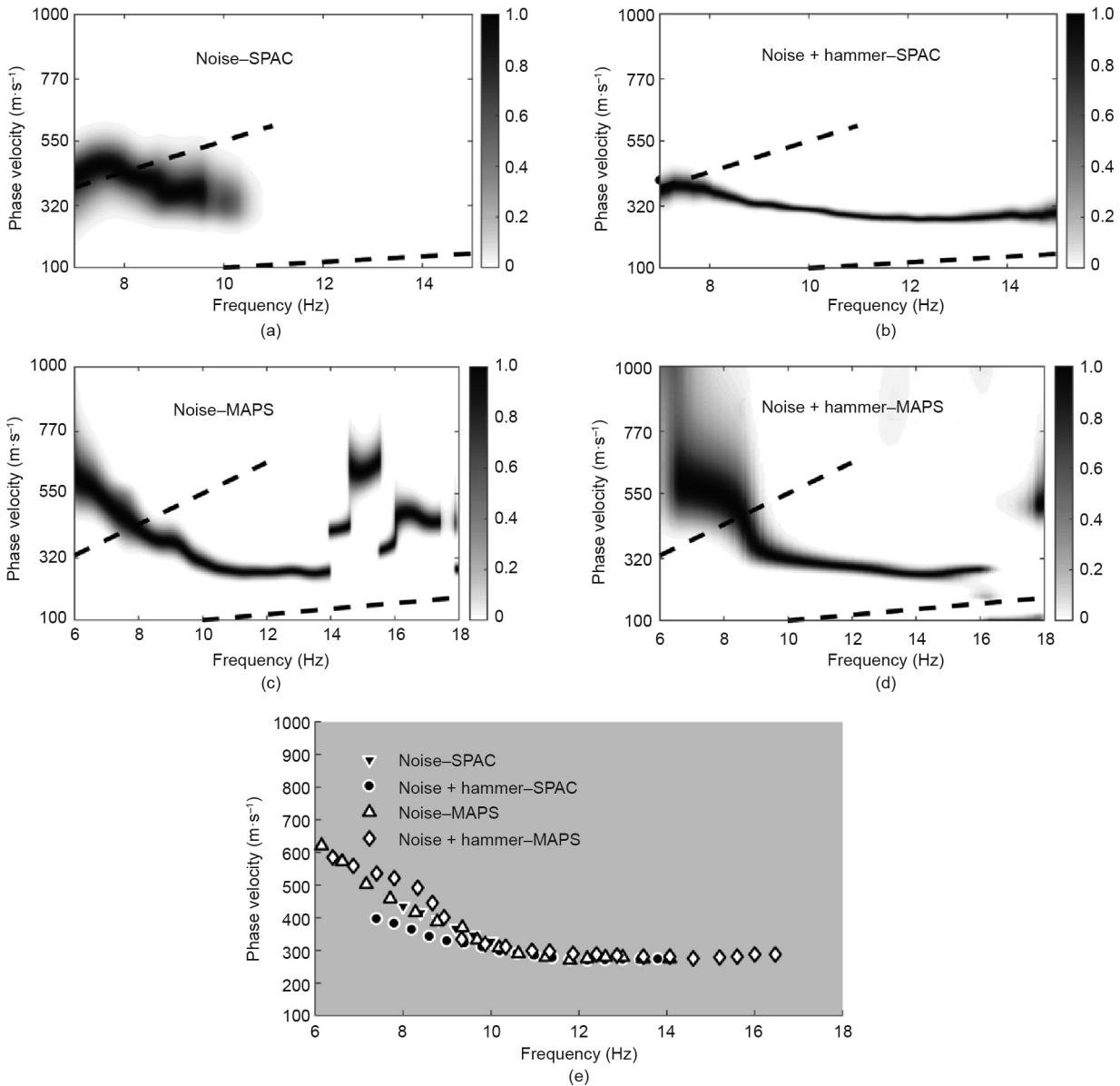

Fig. 9. The average power spectra of (a) the passive surface waves and (b) the MSW.

(Fig. 10(c)) at high frequencies from 14 to 18 Hz, was significantly suppressed in the MSW measurement (Fig. 10(d)); the effect of the coherent energy is discussed later in this paper.

3.3. Site 3: S-level passive surface waves

This test was carried out in the city of Yueyang, China. A linear array with 12 vertical-component receivers of 4.5 Hz each was deployed along the railway from Beijing to Guangzhou, which is one of the busiest railways in China. The trace interval was fixed at 10 m and the sampling rate was 2 ms. In this test, three kinds of noise subsets were recorded and analyzed. The first subset consisted of only "quiet" ambient noise; during the second observation, a passenger train and a freight train sequentially passed; and the third subset consisted of four shots with active sources. The source was a 20 kg rock that was found locally.

Fig. 11 displays the complete noise records of each subset. It is easy to distinguish the arrivals and loads of the two trains (Fig. 11(b)). Spectral analysis was performed on each subset (Fig. 12), and

Fig. 8. (a) One 10 s segment of the passive surface waves from vehicles over a 5 min period; (b) one 10 s segment of the MSW over a 5 min period. The black arrow indicates the active-source shot event.

Fig. 10. (a), (b) The obtained dispersion energy images using the SPAC method; (c), (d) the obtained dispersion energy images using the MAPS method; (e) the picked dispersion curves from (a) to (d). (a) and (c) show the dispersion measurements from the passive surface waves, while (b) and (d) show the measurements from the MSW.
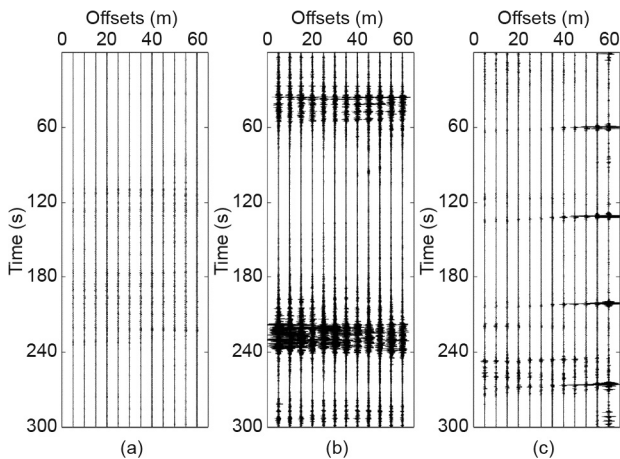

Fig. 11. (a) "Quiet" passive surface waves over a 5 min period; (b) passive surface waves over a 5 min period, with two trains passing by; (c) MSW over a 5 min period, with four rock shots.
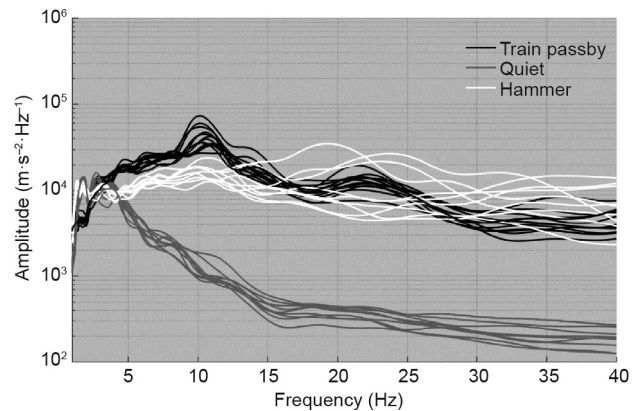
Fig. 12. Power spectra of each trace of the "quiet" passive surface waves (gray lines), MSW (white lines), and passive surface waves with trains passing by (black lines).

indicates that the imposed active sources indeed improved the high-frequency (> 5 Hz) energy of the MSW (white lines), compared with the "quiet" noise (gray lines). The train noise (black lines) showed the highest energy in the frequency range from 5 to 10 Hz, but the powerful high-frequency energy was greatly attenuated above 10 Hz due to the trains' rapid departure. Note that the MSW displays great amplitude fluctuations among these traces with different offsets at high frequency (> 18 Hz), which reveals the effects of geometrical spreading and attenuation.

Dispersion energy images of each subset were obtained using the MAPS method (Fig. 13(a)–(c)) and the SPAC method (Fig. 13(d)–(f)), respectively. The acceptable dispersion curves of the above measurements (Fig. 13(g)) were picked out and fitted well with each other, which corroborated the validity of these measurements. Compared with the "quiet" noise (Fig. 13(a) and (d)), the MSW presents better applicability to high-frequency (>8 Hz) dispersion analysis (Fig. 13(b) and (e)). Although the train noise shows higher amplitude (Fig. 12), the rapid attenuation of the coherent signals at high
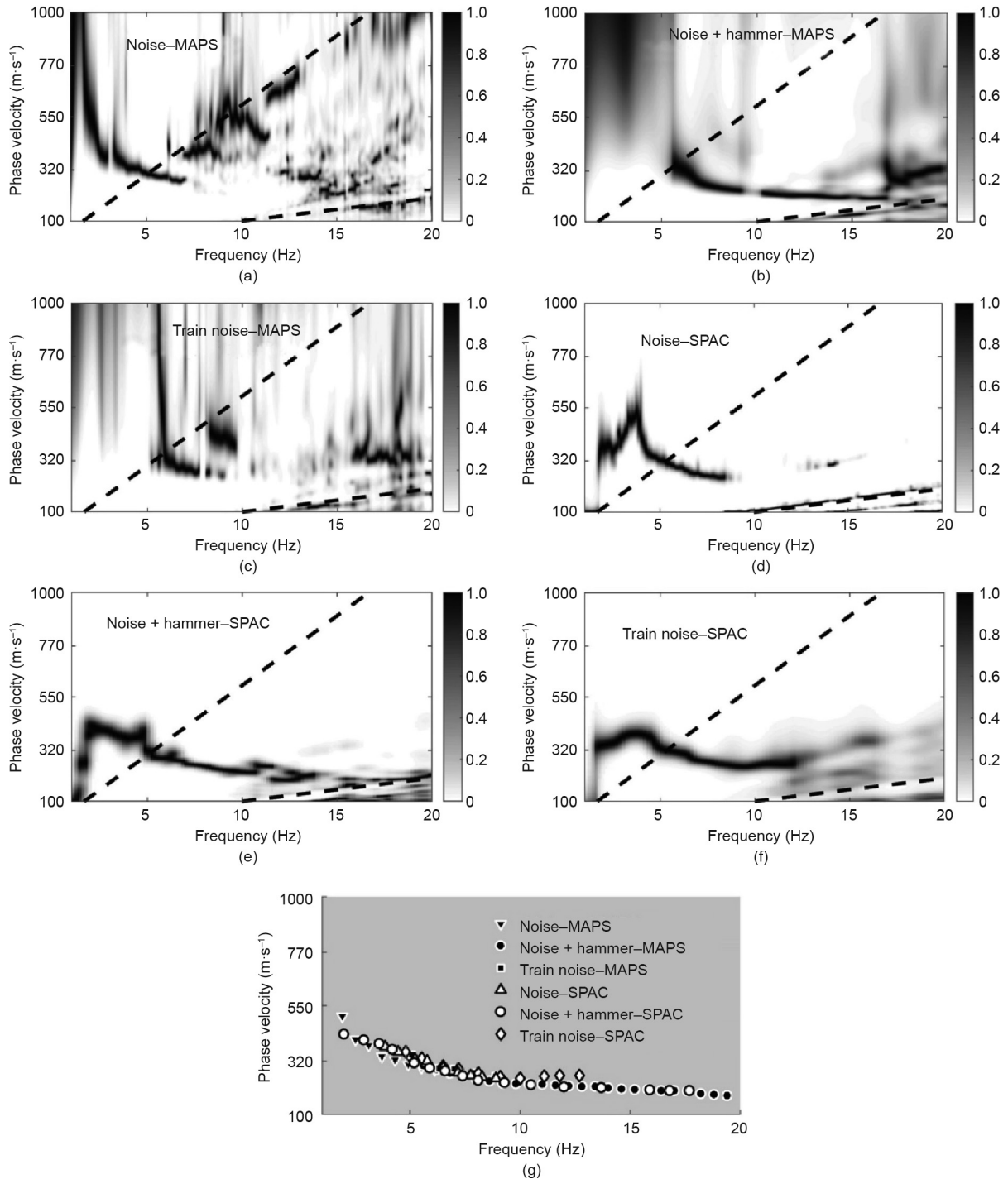
Fig. 13. (a)–(c) The obtained dispersion energy images using the MAPS method; (d)–(f) the obtained dispersion energy images using the SPAC method; (g) the picked dispersion curves from (a) to (f). (a) and (d) show the dispersion measurements from the "quiet" passive surface waves; (b) and (e) show the measurements from the MSW; (c) and (f) show the measurements from the passive surface waves with trains passing by.

frequency (> 10 Hz) makes it extremely difficult to utilize this kind of passive surface wave for high-frequency dispersion analysis (Fig. 13(c) and (f)), which is discussed later.

4. Discussion

Spatial aliasing should always be taken into consideration during passive surface-wave measurement. Utilizing cross-correlations, Cheng et al. [14] demonstrated the advantage of MAPS in suppressing spatial aliasing. Compared with using passive surface waves, we found that the MSW measurement was able to further reduce the effect of spatial aliasing. For example, the MSW measurement (Fig. 5(b)) displays less phase velocity disturbance than the passive surface-wave measurement (Fig. 5(a)) at low frequencies beyond the valid wavenumber zone. In addition, it is easy to find an aliasing energy trend from 7 to 20 Hz (Fig. 13 (a)), whereas the aliasing energy is significantly suppressed in the MSW measurement (Fig. 13(b)). The suppression results from the effect of the coherent energy that is introduced by the active-source shots. It is noticeable that the temporal normalization option during preprocessing will only operate on the amplitude of passive surface waves; it will not affect the coherent phase [29].

Long-duration records used for passive surface-wave measurement not only provide high SNR, but also broaden the period range in which dispersion measurements can be made [30]. However, our results indicate that it is possible to utilize ultrashort-duration records (e.g., several seconds or minutes) for a passive surface-wave survey, rather than long-duration records over several hours or days. Although the use of ultrashort-duration records is beyond the scope of the present work, we suggest that short-duration records will be beneficial in amplifying the coherent energy effect of active-source shots for the MSW measurement due to the SNR weighted stacking operation [25].

The point we wished to emphasize in this paper is that it is possible to obtain higher frequency dispersion information for passive surface-wave methods by imposing active sources during continuous passive surface-wave observation. Therefore, we did not pay much attention to retrieving low-frequency information using passive surface waves in this context. Note that it was difficult to obtain low-frequency (< 5 Hz) phase velocities at Site 3 from MSW and train noise (Fig. 13(b), (c), (e), and (f)) because the powerful sources generated more near-field effects and scatter [31], and ultrashort-duration records (5 min) might be insufficient to ensemble-average this incoherent noise in such a low-frequency range. However, dispersion measurements within the valid wavenumber zone still showed a good performance. This indicates that a longer alignment spread—namely, lowering the lower limit of the wavenumber—is required in order to obtain sufficient depth coverage [32].

Three sites with totally different noise environments were used to demonstrate the flexibility and applicability of the MSW measurement in high-frequency phase velocity analysis. The MSW measurement can also be flexibly implemented in the field. For example, the active source at Site 3 was simply a rock picked on the site ground. It should be mentioned that the effect of the active source (i.e., offsets, weights, frequency, etc.) on the MSW measurement requires further study.

5. Conclusions

This paper proposes a simple procedure for a high-frequency passive surface-wave survey: It is possible to extend the frequency band by imposing active sources during continuous passive surface-wave observation, in a method we call "MSW measurement." We have applied this method at three sites with different noise levels; the results indicate our method's flexibility and applicability in high-frequency phase velocity analysis. Although this preliminary work is not backed up by a theoretical demonstration, the results presented here strongly suggest that it will be constructive to perform MSW measurement during seismic investigation, rather than exclusively performing either active surface-wave measurement or passive surface-wave measurement. The results suggest that the proposed strategy can be an alternative choice in engineering, environmental, and other seismic projects.

Compliance with ethics guidelines

Feng Cheng, Jianghai Xia, Chao Shen, Yue Hu, Zongbo Xu, and Binbin Mi declare that they have no conflict of interest or financial conflicts to disclose.

References

[1] Yoon S. Combined active-passive surface wave measurements at five sites in the western and southern US. KSCE J Civ Eng 2011;15(5):823–30.

[2] Song YY, Castagna JP, Black RA, Knapp RW. Sensitivity of near-surface shear-wave velocity determination from Rayleigh and Love waves. SEG Expanded Abst 1989;8(1):1357.

[3] Park CB, Miller RD, Xia J. Multichannel analysis of surface waves. Geophysics 1999;64(3):800–8.

[4] Xia J, Miller RD, Park CB. Estimation of near-surface shear-wave velocity by inversion of Rayleigh waves. Geophysics 1999;64(3):691–700.

[5] Xia J, Miller RD, Park CB; Kansas Geological Survey. Advantages of calculating shear wave velocity from surface waves with higher modes. In: SEG technical program expanded abstracts 2000. Tulsa: Society of Exploration Geophysicists; 2000. p. 1295–8.

[6] Xia J, Miller RD, Park CB, Tian G. Inversion of high frequency surface waves with fundamental and higher modes. J Appl Geophys 2003;52(1):45–57.

[7] Hayashi K, Suzuki H. CMP cross-correlation analysis of multi-channel surface-wave data. Explor Geophys 2004;35(1):7–13.

[8] Okada H, Suto K. The microtremor survey method. Tulsa: Society of Exploration Geophysicists; 2003.

[9] Aki K. Space and time spectra of stationary stochastic waves, with special reference to micro-tremors. Bull Earthquake Res Inst 1957;35:415–56.

[10] Asten MW. Site shear velocity profile interpretation from microtremor array data by direct fitting of SPAC curves. In: Proceedings of the Third International Symposium on the Effects of Surface Geology on Seismic Motion; 2006 Aug 30–Sep 1; Grenoble, France; 2006.

[11] Xu Y, Zhang B, Luo Y, Xia J. Surface-wave observations after integrating active and passive source data. Leading Edge 2013;32(6):634–7.

[12] Louie JN. Faster, better: shear-wave velocity to 100 meters depth from refraction microtremor arrays. Bull Seismol Soc Am 2001;91(2):347–64.

[13] Park C, Miller R, Laflen D, Neb C, Ivanov J, Bennett B, et al. Imaging dispersion curves of passive surface waves. SEG Expanded Abst 2004;1:1357–60.

[14] Cheng F, Xia J, Luo Y, Xu Z, Wang L, Shen C, et al. Multi-channel analysis of passive surface waves based on cross-correlations. Geophysics 2016;81(5): EN57–66.

[15] Yoon S, Rix GJ. Combined active-passive surface wave measurements for near-surface site characterization. In: Proceedings of the Symposium on the Application of Geophysics to Engineering and Environmental Problems 2004; 2004 Feb 22–26; Colorado Springs, CO. USA. Denver: Environment and Engineering Geophysical Society; 2004. p. 1556–64.

[16] Liu Y, Bay J, Luke B, Louie J, Pullammanappallil S. Combining active- and passive-source measurements to profile shear wave velocities for seismic microzonation. In: Proceedings of the Geo-Frontiers Congress 2005; 2005 Jan 24–26; Austin, TX, USA; 2005.

[17] Park CB, Miller RD, Ryden N, Xia J, Ivanov J. Combined use of active and passive surface waves. J Environ Eng Geophys 2005;10(3):323–34.

[18] Hayashi K, Cakir R, Walsh TJ, State W. Comparison of dispersion curves and velocity models obtained by active and passive surface wave methods. In: Proceedings of the 2016 SEG Annual Meeting; 2016 Oct 16–21; Dallas, TX, USA; 2016. p. 4983–8.

[19] Aki K. A note on the use of microseisms in determining the shallow structures of the earth's crust. Geophysics 1965;30(4):665–6.

[20] Ohori M, Nobata A, Wakamatsu K. A comparison of ESAC and FK methods of estimating phase velocity using arbitrarily shaped microtremor arrays. Bull Seismol Soc Am 2002;92(6):2323–32.

[21] Weemstra C, Boschi L, Goertz A, Artman B. Seismic attenuation from recordings of ambient noise. Geophysics 2013;78(1):Q1–14.

[22] Asten MW. On bias and noise in passive seismic data from finite circular array data processed using SPAC methods. Geophysics 2006;71(6):V153–62.

[23] Chávez-García FJ, Luzón F. On the correlation of seismic microtremors. J Geophys Res 2005;110:1–12.

[24] Chávez-García FJ, Rodríguez M, Stephenson WR. Subsoil structure using SPAC measurements along a line. Bull Seismol Soc Am 2006;96(2):729–36.

[25] Cheng F, Xia J, Xu Y, Xu Z, Pan Y. A new passive seismic method based on seismic interferometry and multichannel analysis of surface waves. J Appl Geophys 2015;117:126–35.

[26] Luo Y, Xia J, Miller RD, Xu Y, Liu J, Liu Q. Rayleigh-wave dispersive energy imaging using a high-resolution linear radon transform. Pure Appl Geophys 2008;165(5):903–22.

[27] Xia J, Xu Y, Chen C, Kaufmann RD, Luo Y. Simple equations guide high-frequency surface-wave investigation techniques. Soil Dyn Earthquake Eng 2006;26(5):395–403.

[28] Pan Y, Xia J, Zeng C. Verification of correctness of using real part of complex root as Rayleigh-wave phase velocity with synthetic data. J Appl Geophys 2013;88:94–100.

[29] Bensen GD, Ritzwoller MH, Barmin MP, Levshin AL, Lin F, Moschetti MP, et al. Processing seismic ambient noise data to obtain reliable broad-band surface wave dispersion measurements. Geophys J Int 2007;169 (3):1239–60.

[30] Chimoto K, Yamanaka H. Effects of the durations of crosscorrelated microtremor records on broadband dispersion measurements using seismic interferometry. Geophysics 2014;79(3):Q11–9.

[31] Yoon S, Rix GJ. Near-field effects on array-based surface wave methods with active sources. J Geotech Geoenviron Eng 2009;135(3): 399–406.

[32] Lin CP, Lin CH. Effect of lateral heterogeneity on surface wave testing: numerical simulations and a countermeasure. Soil Dyn Earthquake Eng 2007;27(6):541–52.